Supporting Information for

Tetrahedron Structured DNA and Functional Oligonucleotide for Construction of Electrochemical DNA-Based Biosensor

Nan-Nan Bu, Chun-Xia Tang, Xi-Wen He, Xue-Bo Yin*

Research Center for Analytical Sciences,

College of Chemistry, Nankai University, Tianjin 300071, China

E-mail: xbyin@nankai.edu.cn

Contents:

1. Experimental Section

Apparatus. The electrochemical measurements for differential pulse voltammetry (DPV) and cyclic voltammetry (CV) were carried out using an Electrochemical Analyzer (Ivium Technologies, Netherlands) with a standard three-electrode system with Ag/AgCl/KCl (sat) as reference electrode, 2 mm diameter DNA-modified Au electrode as working electrode, and Pt wire as counter electrode. All electrochemical measures were performed at room temperature in 20 mM Tris-HCl (pH 7.0) containing 0.1 M NaCl. DPV was recorded within the potential range from 0 to -0.4 V at pulse amplitude of 10 mV and a scan rate of 20 mV s^{-1} with a step potential of 10 mV. CV was conducted at a scan rate of 100 mV s^{-1} between -0.5 V and 0.4 V.

Chemicals and materials. The sequence of the four oligonucleotides (TS-a, TS-b, TS-c, TS-d) for formation tertrhedron-structured part was reported previously. [S1] All of the oligonucleotides used for construction of Hg^{2+} ion biosensor were prepared by Takara Biotechnology (Dalian, China). The sequences of the oligomers used were:

1: 5'-SH-(CH$_2$)$_6$-*TTTTT*-3' (SS1) (The black italic T$_5$ is the section for Hg^{2+} ion identification)

2: 3'-GGGGG TTTTT-5' (This functional oligonucleotide (denoted as FO) acts for Hg^{2+} ion identification and MB introduction. G$_5$ is used to introduce MB as the signal molecule and T$_5$ is used to form T-Hg-T construction with the black italic T$_5$ in SS1 or TS-a.)

3: 5'-AAAAA-3' (SS2)

4: 5'-*TTTTT* ACATT CCTAA GTCTG AAACA TTACA GCTTG CTACA CGAGA AGAGC CGCCA TAGTA-3' (TS-a) (The black italic T$_5$ is the section for Hg^{2+} ion identification)

5: 5'-SH-C$_6$-TATCA CCAGG CAGTT GACAG TGTAG CAAGC TGTAA TAGAT GCGAG GGTCC AATAC-3' (TS-b)

6: 5'-SH-C$_6$-TCAAC TGCCT GGTGA TAAAA CGACA CTACG TGGGA ATCTA CTATG GCGGC

TCTTC-3' (TS-c)

7: 5'-SH-C$_6$-TTCAG ACTTA GGAAT GTGCT TCCCA CGTAG TGTCG TTTGT ATTGG ACCCT CGCAT-3' (TS-d)

The oligonucleotides were prepared into 5 µM in TE buffer (10 mM Tris-HCl, 1 mM EDTA, pH 7.5) as their single-stranded concentration. The four DNA strands (TS-a, TS-b, TS-c, and TS-d) were mixed equimolar quantities in TE buffer (10 mM Tris-HCl, 1 mM EDTA, pH 7.5), heated the mixture to 95 °C for 2 min and then cooled to 4 °C in 30 s to form tetrahedron-structured DNA. [S1] 2-mercaptoethanol (MCE) used to block the sensing interface for detection, was obtained from Yangguang Yunneng Biotechnology Company, Tianjin, China. The 2 mm diameter Au disk electrode was obtained from Tianjin Lanlike High-Tech Company (Tianjin, China). Saline solutions were prepared with Mn(Ac)$_2$, Mg(NO$_3$)$_2$, Pb(NO$_3$)$_2$, Zn(Ac)$_2$, Cd(NO$_3$)$_2$, Fe(NO$_3$)$_3$, CaCl$_2$, Co(Ac)$_2$, Cu(NO$_3$)$_2$, and Hg(NO$_3$)$_2$. Milli-Q ultra-pure water was used in each experiment. The Tris-HCl solution is used as detection electrolyte.

Procedure of Sensing Hg^{2+}. The clean gold electrodes were incubated with 1µM ts-DNA over night at room temperature for immobilization of ts-DNA. Then, the modified electrode was thoroughly rinsed with 20 mM Tris-HCl buffer and water to remove the weakly adsorbed ts-DNA. At the same time, 10 µM FO ss-DNA (SS2) was mixed with 2 mM MB for the probe introduction at room temperature for 2 hours, 10 µM ss-DNA (SS2) was further added into the MB-labeled ss-DNA for the formation of A-T double helix structure for 1 hour at 36 °C. To determine the Hg^{2+} in sample, 4 µL MB integrated oligomer (MB-FO) and 10 µL of the Hg^{2+} ions with various concentrations was incubated on the ts-DNA-modified electrode for 1 hour at 36 °C. The formation of T-Hg^{2+}-T complex achieved the introduction of MB onto the electrode surface. The electrode was washed thoroughly with ultrapure water and 20 mM Tris-HCl buffer to reduce the nonspecific binding. To validate the efficiency of ts-DNA for the sensing Hg^{2+}, the gold electrode surface was not blocked with 10 µL of 0.1 M MCE solution different to the use of linear ss-DNA. The selectivity of the biosensor was tested in the presence of the competing metal ions such as Mn^{2+}, Mg^{2+}, Pb^{2+}, Zn^{2+}, Cd^{2+}, Fe^{3+}, Ca^{2+}, Co^{2+} and Cu^{2+}.

As a comparison, linear ss-DNA (SS1) was used to introduce the Hg^{2+} ion identification section, T_5 with the electrode was soaked in 5 μm thiolated oligonucleotide (SS1) solution over night at room temperature instead of ts-DNA. After blocking the active site of the ss-DNA-modified electrode with 10 μL of 0.1 M MCE, the other procedures for determination of Hg^{2+} were same as those using ts-DNA-modified electrode.

2. Construction of the DNA biosensor for Hg^{2+}

The biosensor for Hg^{2+} ions described here includes three parts: preparation and assembly of ts-DNA used to introduce a T_5 DNA section for Hg^{2+} ion identification; the functional oligonucleotide (FO) designed for Hg^{2+} ion identification and the introduction of the electrochemical probe, MB, via the interaction between MB and a DNA strand; the formation of thymine-Hg^{2+}-thymine complex (T-Hg^{2+}-T).

The ts-DNA was hierarchically assembled from three thiolated DNA strands (TS-b, TS-c, and TS-d), each of which contained 55 nucleotides (55-nt), and a DNA fragment (TS-a) of 60 nucleotide (60-nt) as shown in Scheme 1A. [S1] The ts-DNA was anchored to the electrode surface through the thiol end by incubation of gold electrode with 1 μM ts-DNA. The 60-nt DNA fragment contained a section to form ts-DNA and T_5 section for Hg^{2+} ion identification. The coordination reaction between Hg^{2+} and thymine bases at ts-DNA and FO provided a selective platform for the capture of Hg^{2+} through the formation stable DNA duplexes, T-Hg^{2+}-T. [S2]

The FO was designed to contain two functional sections. Five thymidine bases (T_5) comprised the Hg^{2+} identification section, which formed T-Hg^{2+}-T construct with the immobilized T_5 in ts-DNA or SS2. The probe introduction section was an oligonucleotide section of five guanine bases as shown in the sequence of SS2. Two multi-thymidine DNA strands are able to form strong and stable T-Hg^{2+}-T base pairs with a binding constant (Kd) of 4.14×10^6 L mol^{-1}, which is higher than that of A-T. [S2]

Single- and double-stranded DNA have the capacity to incorporate a variety of small molecules via electrostatic interaction or by intercalation into the groove of ds-DNA. [S3] By intercalation of Ru(phen)$_3^{2+}$ into ds-DNA, a series of DNA-based biosensors were developed by our group for detecting thrombin, [S3e] lysozyme, [S3e-g] and for probing Hg^{2+}. [S2a] In addition to tagging MB onto the end of DNA strand for the development of biosensors, [S4] it has also been shown that MB can bind specifically to guanine base and is readily intercalated into ds-DNA. [S5] The signal change of MB before and after interaction to DNA strand was used to develop DNA-based biosensors, which eliminated the covalent

chemical labelling step. [S4-S6] Moreover, because more than one MB molecule is able to interact with the DNA strand, the efficiency of probe introduction is much higher than the single-site labelling techniques. [S3]

The construction of biosensor for Hg^{2+} ions with ts-DNA was performed as shown in Scheme 1A. The ts-DNA was used to introduce the Hg^{2+} ion identification section, T_5. After FO was integrated with MB (denoted as MB-FO, Scheme 1C), it formed T-Hg^{2+}-T complex by interaction of T_5 and Hg^{2+} ions. The electrochemical signal from MB was used to quantify Hg^{2+} ions. No syntheses of chemically modified oligonucleotides are required for this approach, which is simpler, faster, and more economical than other methods. [S7] The "turn-on" mode of this sensor also means it does not suffer from the problems of false positives and limited signal intensity that are features in the "turn-off" systems. [S8] Because the MB-FO complex was pre-prepared as shown in Scheme 1C, the time taken for each assay only included the incubation time for sample and MB-FO complex on the electrode surface and the analysis time. For comparison, linear ss-DNA was used to immobilize the Hg^{2+} ion identification section, T_5, on the electrode for the formation of T-Hg^{2+}-T. The MB probe was introduced onto the electrode surface for electrochemical characterization of the response to Hg^{2+} ions, as shown in Scheme 1B.

3. The electrochemistry of MB integrated into DNA for sensing Hg^{2+}

To validate the possibility of MB integrated into DNA for sensing Hg^{2+}, linear ssDNA was first used to introduce T$_5$, the Hg^{2+} ion identification section (Scheme 1B). After blocking with mercaptoethanol (MCE), a mixture of 10 μL of sample and 4 μL of MB-FO (Scheme 1C) was dropped onto the T$_5$-modified Au electrode. Formation of the T-Hg^{2+}-T construct resulted in the introduction of the probe, MB, onto the electrode surface. An electrochemical signal was recorded as shown in Fig. S1. No obvious redox peak was observed at the T$_5$-modified electrode (Fig. S1Aa and S1Ba). However, once the MB-DNA complex was introduced onto the electrode surface through the formation of the T-Hg^{2+}-T complex, redox peaks were observed at ca. -0.2 V (Fig. S1Ab and S1Bb). Fig. S2 shows cyclic voltammetry (CV) and differential pulse voltammetry (DPV) records from the bare gold electrode in 1 mM MB solution. A pair of redox peaks appeared at the CV curve and the potential for reduce peak was at about -0.2 V as shown in Figure S2A. The same peak potential to that from the present Hg^{2+} biosensors indicates that the redox peaks in Figure 1Ab resulted from MB and confirmed that the probe, MB molecules, was introduced onto the electrode surface. Although Hg^{2+} ions are able to interact with thiol groups, they do not destroy the thiol-gold bond used to immobilize the T$_5$ onto the electrode surface.
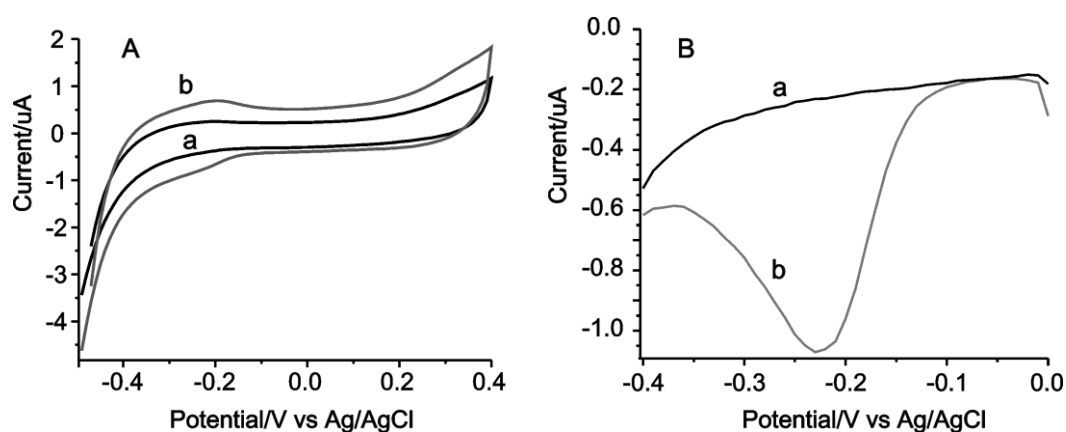

Fig. S1. Cyclic voltammetry (A) and differential pulse voltammetry (B) of T$_5$-modified electrode before (a) and after (b) being incubated with 10 μL 600 nM Hg^{2+} ions plus 4 μL MB integrated oligonucleotide

(SS2) in 20 mM Tris-HCl (pH 7.0, 0.1 M NaCl). Conditions: (A) scan rate: 50 mV s^{-1}; (B) pulse amplitude of 10 mV and scan rate of 20 mV s^{-1} with a step potential of 10 mV.
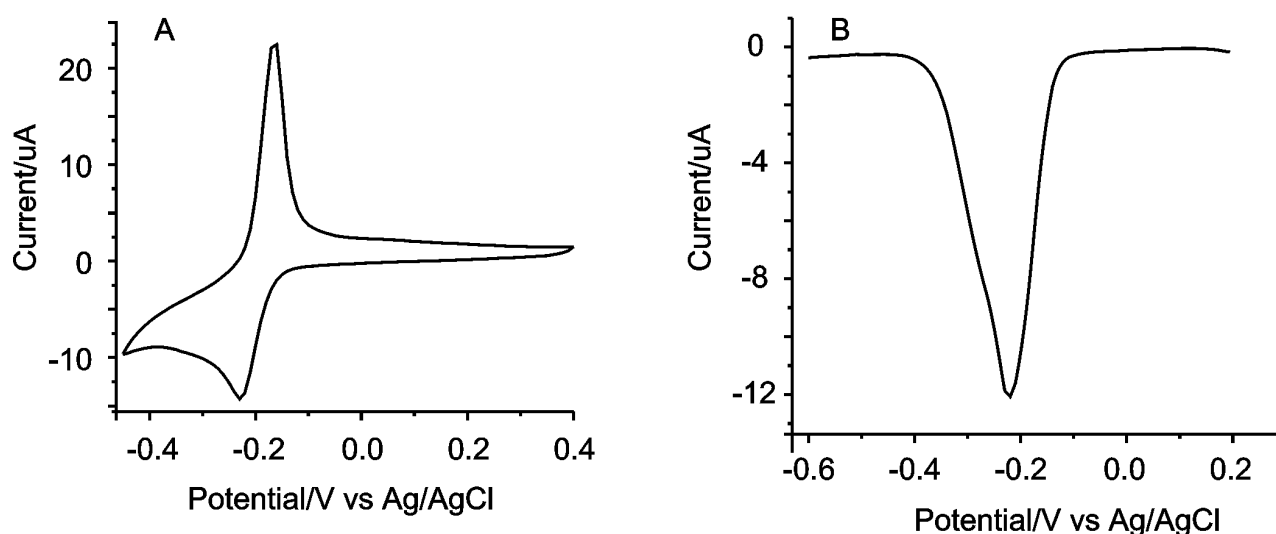

Fig. S2 Cyclic voltammetry (A) and differential pulse voltammetry (B) of 1 mM methylene blue at bare gold electrode in 20 mM Tris-HCl buffer containing. Condition: (A) scan rate: 0.1 V s^{-1}. (B) scan rate: 20 mV s^{-1} with a step potential of 10 mV.

Differential pulse voltammetry (DPV) is able to provide well-resolved voltammograms with fine-scale current resolution and negligible charging current compared with CV. Fig. S1B shows the cathodic current at T$_5$-modified electrode before and after being incubated with a mixture of 10 μL 600 nM Hg^{2+} ions and 4 μL MB-FO using linear ss-DNA. In comparison with the current in Fig. S1A, an improved cathodic current was observed. The amplitude of the applied potential was increased linearly. Use of single pulse prevented a faradic reaction because the faradic current decayed with the square root of time. Thus, the current was collected at a time within the pulse width while the charging current was negligible. DPV was therefore used to quantify the content of Hg^{2+} ions in the further work because of its improved sensitivity.

Cyclic voltammetry at a range of scan rates was used to investigate the electrochemistry of MB introduced through the formation of the T-Hg^{2+}-T complex with the probe introduction section. The anodic peak currents, *Ipc*, of MB oxidation (Fig. S3A) were directly proportional to the scan rates (Fig. S3B). The results indicated that MB oxidation was a surface-controlled process. Combining the result in

Fig. S1 and S3, we could conclude that MB was stably attached to the probe introduction section and

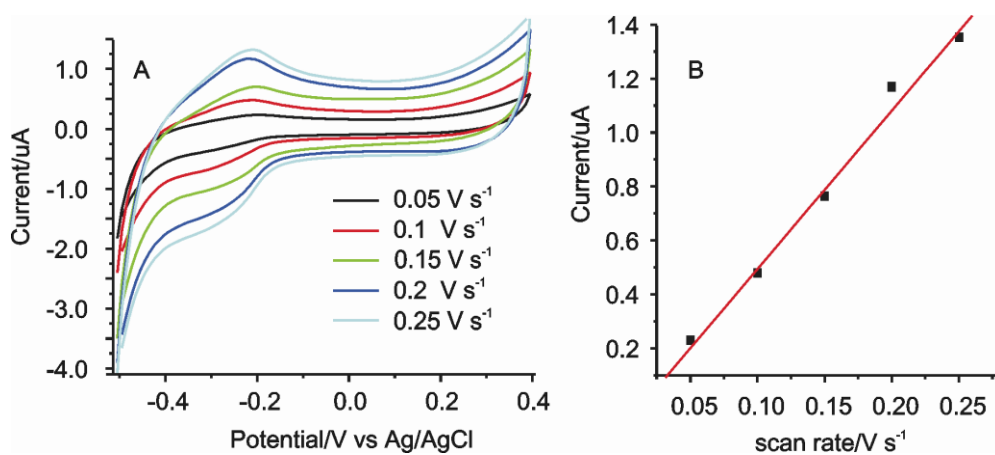was introduced into the electrode surface through the formation of T-Hg^{2+}-T complex.

Fig. S3 (A) Cyclic voltammograms at different scan rates after the introduction of methylene blue to the

electrode via the formation of a T-Hg^{2+}-T duplex with the probe introduction DNA. (B) The relationship

between the first anodic peak currents and the scan rates.

4. The response of the biosensor with and without the hybridization of Hg^{2+} identification section to A_5

A section of oligonucleotide, A_5 (SS2), was used to pre-form ds-DNA with the Hg^{2+} identification section to avoid coupling of Hg^{2+} ions and two FO strands via their Hg identification sections. The effects on the electrochemical signal with and without the pre-formed hybrid between A_5 and FO complex were tested. As shown in Figure S4, an obviously low signal (0.483 vs 0.684 μA) was observed if no the hybrid pre-formed for 600 nM Hg^+ ions. Moreover, the reproducibility was poor. Hg^{2+} ions can form $T-Hg^{2+}-T$ duplex with two FO oligonucleotide molecules via their Hg^{2+} identification sections. This interaction decreases the introduction of the MB labeled DNA complex into the electrode surface. However, if the Hg^{2+} identification section in FO formed the hybrid with A_5, The competitive binding leads to the high and reproducible ECL emission because of the binding constant (K_b) of $T-Hg^{2+}-T$ is 4.14×10^6 L mol^{-1}, which is higher than that of the A-T complex. [S2e] The competitive result makes Hg^{2+} ions is prone to hybridize the immobilized T_5 and SS2 labeled with MB. While the pre-formed A-T duplex in FO strand prevents the interaction between Hg^{2+} ions and two FO oligonucleotide molecules, it does not affect coupling of the immobilized T_5 and FO via Hg^{2+} ions (Fig. S4). Because MB interacts with guanine bases, [S9] the formation of this complex does not affect the formation of $T-Hg^{2+}-T$. The results show that the Hg^{2+} identification section and probe introduction section do not interfere with each other.
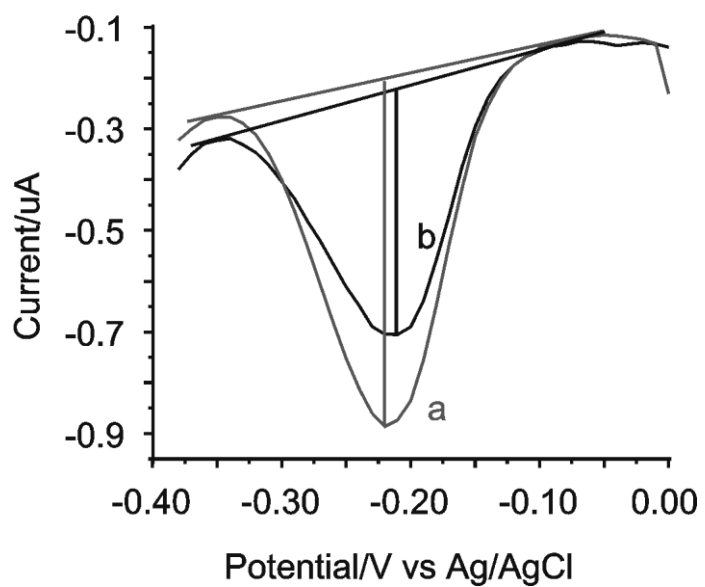
Fig. S4 Differential pulse voltammetry of the biosensor for Hg^{2+} with (a) and without (b) the pre-formed part duplex between SS2 and FO.
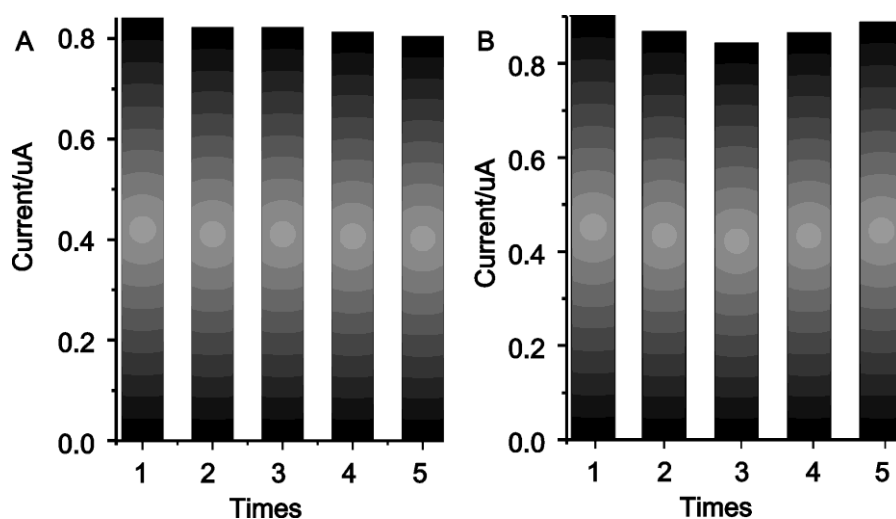
Fig. S5 The signal intensity for five replicate determinations of (A) 10 nM Hg^{2+} ion by the use of ts-DNA with RSD of 1.7 % and (B) of 50 nM Hg^{2+} ion by the use of ss-DNA with RSD of 2.6 %.
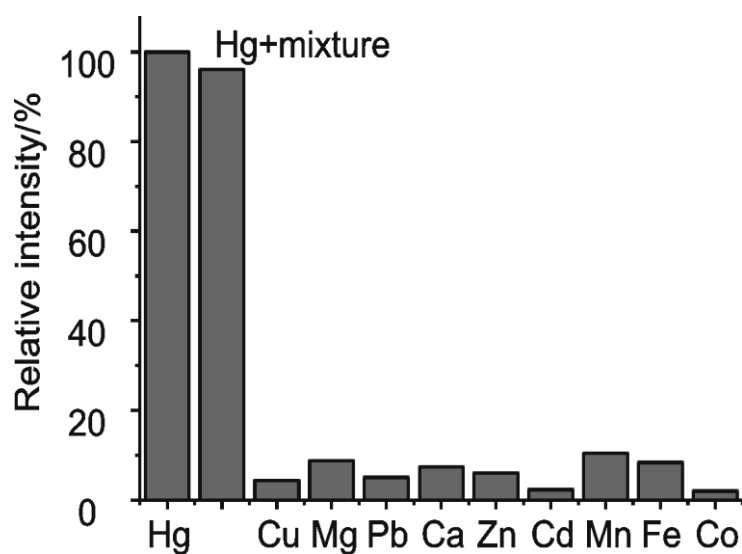

Fig. S6 Selectivity of the Hg^{2+} ion biosensor. Competing ion solutions were tested at 10 μM. For comparison, the responses from 10 nM Hg^{2+} ions, and from the mixtures of 10 nM Hg^{2+} with 1μM of each of ions were shown.

Table S1. Method detection limits (DLs) for Hg^{2+} ions using different oligonucleotide -based techniques.

Method	Notes	Sensing mode	DL/nM [b]	Ref.
EC [a]	Tetrahedron Structured DNA for immobilization of Hg identification section	Turn-on	0.1	This work
ECL [a]	A functional oligonucleotide containing Hg identification section and ECL probe intercalation section	Turn-on	0.02	S2a
ECL	$Ru(bpy)_3^{2+}$-doped silica nanoparticles labeled DNA	Turn-on	2.3	S2e
EC	The signal from Hg^{2+} reduced to Hg^+ in combination with Au nanoparticle amplification	Turn-off	0.5	S2c
Optics	Optical sensing with a conjugated polymer using its coupling to T-Hg^{2+}-T	Turn-on	42	S2h
FL [a]	UO_2^{2+}-specific DNAzyme for the enhanced fluorescence	Turn-on	2.4	S8a
FL	Fluorescence from Au nanoparticles using the different electrostatic affinity between ss-DNA and ds-DNA	Turn-on	40	S8b
FL	The formation of T-Hg^{2+}-T results in the quench to fluorophore	Turn-off	40	S8c
FL	Enhanced fluorescence from TOTO-3 intercalated into T-Hg^{2+}-T	Turn-on	0.6 ppb	S8d
FL	Simultaneous determination of Hg^{2+} and Ag^+ by nucleic acid functionalized quantum dots.	Turn-off	10	S8h
Colorimetry	Hg^{2+}-induced aggregation of DNA-functionalized Au nanoparticles	Turn-off	10	S8g
Colorimetry	The formation of T-Hg^{2+}-T inhibits the G-quadruplex DNAzyme activity	Turn-off	50	S10
Colorimetry	The formation of T-Hg^{2+}-T inhibits the G-quadruplex DNAzyme activity	Turn-off	4.5	S11
Colorimetry	The formation of T-Hg^{2+}-T inhibits the G-quadruplex DNAzyme activity	Turn-off	100	S12
Colorimetry	Hg^{2+}-induced aggregation of DNA-functionalized Au nanoparticles	Turn-on	250	S13
Colorimetry	The UV absorbance from the intermolecular four-stranded G-quadruplex–hemin complexes induced by Hg^{2+}	Turn-on	52	S14
Colorimetry	The UV absorbance from split G-quadruplex–hemin complexes induced by Hg^{2+}	Turn-on	19	S15

[a] ECL: electrochemiluminescence; EC: electrochemistry; FL: fluorescence method.

[b] 1 nM corresponds to ca 0.2 ppb or 0.2 µg L^{-1}.

Table S2. Comparison of analytical results of Hg^{2+} ions in water samples obtained using the present electrochemical biosensor and by cold vapor atomic absorption spectroscopy (CV-AAS).

	Added Conc. (nM)	Conc. Found (nM)	Recovery/%	RSD/%, n=3	CV-AAS (nM) [a]
Tap water	0	n.d.[b]	--		n.d.
	5.00	4.84	96.8	4.2	--
	80.0	76.38	95.4	1.1	--
Lake water	0	3.03	--	--	2.98
	5.00	8.47	109	1.8	--
	80.0	89.57	108	1.5	--
River water	0	1.83	--	--	1.88
	5.00	6.72	97.8	3.4	--
	80.0	84.94	104	3.7	--

[a] 10 mL of sample needed for each determination with CV-AAS, and only 10 μL needed for the present electrochemical biosensor. [b] n.d. not detectable.

Table 3. Comparison of analytical performance for Hg^{2+} ions by the use of ts-DNA and ss-DNA-based sensor.

	ss-DNA-based sensor	ts-DNA-based sensor
Detection limit	10 nM	100 pM
Precision(RSD, n=5)	2.57 %	1.69 %

Supplementary References

S1. H. Pei, N. Lu, Y. L. Wen, S. P. Song, Y. Liu, H. Yan, C. H. Fan, *Adv. Mater.* **2010**, *22*, 4754-4758.

S2. a) C. X. Tang, Y. Zhao, X. W. He, X. B. Yin, *Chem. Comm.*, **2010**, *46*, 9022-9024. b) D. H. Han, Y. R. Kim, J. W. Oh, T. H. Kim, R. K. Mahajan, J. S. Kim, H. Kim, *Analyst*, **2009**, *134*, 1857–1862. c) Z. Q. Zhu, Y. Y. Su, J. Li, D. Li, J. Zhang, S. P. Song, Y. Zhao, G. X. Li, C. H. Fan, *Anal. Chem.*, **2009**, *81*, 7660–7666. d) Y. Xu, L. Yang, X. Y. Ye, P. G. He, Y. Z. Fang, *Electroanalysis*, **2006**, *18*, 1449-1456. e) X. Zhu, L. F. Chen, Z. Y. Lin, B. Qiu, G. N. Chen, *Chem. Commun.* **2010,** *46*, 3149-3151. f) J. S. Lee, M. S. Han, C. A. Mirkin, *Angew. Chem. Int. Ed.* **2007**, *46*, 4093-4096. g) S. J. Liu, G. H. Nie, J. H. Jiang, G. L. Shen, R. Q. Yu, *Anal. Chem.* **2009**, *81*, 5724-5730. h) X. F. Liu, Y. L. Tang, L. H. Wang, J. Zhang, S. P. Song, C. H. Fan, S. Wang, *Adv. Mater.* **2007***, 19*, 1471-1474.

S3. a) B. L. Li, H. Wei, S. J. Dong, *Chem. Comm.* **2007**, 73-75. b) J. Wang, Y. X. Jiang, C. S. Zhou, X. H. Fang, *Anal. Chem.* **2005**, *77*, 3542-3546. c) Y. Jiang, X. X. H. Fang, C. L. Bai, *Anal. Chem.* **2004**, *76*, 5230-5235. d) C. C. Huang, S. H. Chiu, Y. F. Huang, H. T. Chang, *Anal. Chem.* **2007**, *79*, 4798-4804. e) X. B. Yin, Y. Y. Xin, Y. Zhao, *Anal. Chem.* **2009**, *81*, 9299-9305. f) D. Y. Liu, Y. Y. Xin, X. W. He, X. B. Yin, *Analyst*, **2011**, *136*, 478-485. g) D. Y. Liu, Y. Y. Xin, X. W. He, X. B. Yin, *Biosens. Bioelectron.* **2011**, *26*, 2703-2706.

S4. A. A. Rowe, E. A. Miller, K. W. Plaxco, *Anal. Chem.* **2010**, *82*, 7090–7095.

S5. a) C. C. Huang, S. H. Chiu, Y. F. Huang, H. T. Chang, *Anal. Chem.* **2007**, *79*, 4798–4804. b) Y. Jin, X. Yao, Q. Liu, J. H. Li, *Biosens. Bioelectron.* **2007**, *22*, 1126-1130.

S6. Z. X. Zhang, X. L. Wang, Y. Wang, X. R. Yang, *Analyst*, **2010**, *135*, 2960-2964.

S7. a) E. Paleček, *Electroanalysis*, **2009**, *21*, 239-251. b) A. Sassolas, L. J. Blum, B. D. Leca-Bouvier, *Electroanalysis*, **2009**, *21*, 1237-1250. c) Y. Xiao, T. Uzawa, R. J. White, D. DeMartini, K. W. Plaxco, *Electroanalysis*, **2009**, *21*, 1267-1271. d) Y. Xiao, A. A. Lubin, A. J. Heeger, K. W. Plaxco, *Angew. Chem. Int. Ed.*, **2005**, *44*, 5456-5459.

S8. a) J. W. Liu, Y. Lu, *Angew. Chem. Int. Ed.* **2007***, 46*, 7587 –7590. b) H. Wang, Y. X. Wang, J. Y. Jin, R. H. Yang, *Anal. Chem.* **2008**, *80*, 9021-9028. c) A. Ono, H. Togashi, *Angew. Chem. Int. Ed.* **2004**, *43*, 4300-4302. d) C. K. Chiang, C. C. Huang, C. W. Liu, H. T. Chang, *Anal. Chem.* **2008**, *80*, 3716-3721. e) S. Yoon, E. W. Miller, Q. W. He, P. H. Do, C. J. Chang, *Angew. Chem. Int. Ed.* **2007***, 46*, 6658-6661. f) Y. Miyake, H. Togashi, M. Tashiro, H. Yamaguchi, S. Oda, M. Kudo, Y. Tanaka, Y. Kondo, R. Sawa, T. Fujimoto, T. Machinami, A. Ono, *J. Am. Chem. Soc.* **2006**, *128*, 2172-2173. g) D. Li, A. Wieckowska, I. Willner, *Angew. Chem. Int. Ed.* **2008***, 47*, 3927-3931. h) R. Freeman, T. Finder, I. Willner, *Angew. Chem. Int. Ed.* **2009***, 48*, 7818-7821.

S9. a) B. L. Li, H. Wei, S. J. Dong, *Chem. Comm.* **2007**, 73-75. b) J. Wang, Y. X. Jiang, C. S. Zhou, X. H. Fang, *Anal. Chem.* **2005**, *77*, 3542-3546. c) Y. Jiang, X. X. H. Fang, C. L. Bai, *Anal. Chem.* **2004**,

76, 5230-5235. d) C. C. Huang, S. H. Chiu, Y. F. Huang, H. T. Chang, *Anal. Chem.* **2007**, *79*, 4798-4804. e) X. B. Yin, Y. Y. Xin, Y. Zhao, *Anal. Chem.* **2009**, *81*, 9299-9305. f) D. Y. Liu, Y. Y. Xin, X. W. He, X. B. Yin, *Analyst*, **2011**, *136*, 478-485. h) D. Y. Liu, Y. Y. Xin, X. W. He, X. B. Yin, *Biosens. Bioelectron.* **2011**, *26*, 2703-2706.

S10.   T. Li, S. J. Dong, E. K. Wang, *Anal. Chem.* **2009***, 81*, 2144-2149.

S11.   N. Lu, C. Y. Shao, Z. X. Deng, *Analyst* **2009***, 134*, 1822-1825.

S12.   T. Li, B. L. Li, S. J. Dong, E. K. Wang, *Chem. Commun.* **2009**, 3551–3553.

S13.   C. W. Liu, Y. T. Hsieh, C. C. Huang, Z. H. Lin, H. T. Chang, *Chem. Commun.,* **2008,** 2242–2244.

S14.   D. M. Kong, J. Wu, N. Wang, W. Yang, H. X. Shen, *Talanta*, **2009**, *80*, 459-465.

S15.   D. M. Kong, Wang, N. X. X. Guo, H. X. Shen, *Analst*, **2010**, *135*, 545-549.